TRIGGERING AND ENERGETICS OF A SINGLE DROP VAPOR EXPLOSION: THE ROLE OF ENTRAPPED NON-CONDENSABLE GASES

ROBERTA CONCILIO HANSSON
Division of Nuclear Power Safety, Royal Institute of Technology
AlbaNova Center, Division of Nuclear Power Safety, 106 91 Stockholm, Sweden
E-mail : tita@safety.sci.kth.se

Received January 12, 2009
Accepted September 1, 2009

The present work pertains to a research program to study Molten Fuel-Coolant Interactions (MFCI), which may occur in a nuclear power plant during a hypothetical severe accident. Dynamics of the hot liquid (melt) droplet and the volatile liquid (coolant) were investigated in the MISTEE (Micro-Interactions in Steam Explosion Experiments) facility by performing well-controlled, externally triggered, single-droplet experiments, using a high-speed visualization system with synchronized digital cinematography and continuous X-ray radiography.

The current study is concerned with the MISTEE-NCG test campaign, in which a considerable amount of non-condensable gases (NCG) are present in the film that enfolds the molten droplet. The SHARP images for the MISTEE-NCG tests were analyzed and special attention was given to the morphology (aspect ratio) and dynamics of the air/ vapor bubble, as well as the melt drop preconditioning. Energetics of the vapor explosion (conversion ratio) were also evaluated.

The MISTEE–NCG tests showed two main aspects when compared to the MISTEE test series (without entrapped air). First, analysis showed that the melt preconditioning still strongly depends on the coolant subcooling. Second, in respect to the energetics, the tests consistently showed a reduced conversion ratio compared to that of the MISTEE test series.

KEYWORDS : Fuel-Coolant Interactions, Non-Condensable Gases, Preconditioning, X-ray Radiography

1. INTRODUCTION

Molten Fuel-Coolant Interactions (MFCI), which may occur in a nuclear power plant during a hypothetical severe accident, under certain conditions might lead to energetic vapor explosions that challenge the structural integrity of the plant safety barriers. Namely, the high-temperature molten corium, discharged into a water pool, fragments into melt droplets, which are surrounded by a vapor film in a film-boiling regime. Triggered, the vapor film may collapse to allow melt-coolant contact, leading to the melt's rapid fragmentation, which creates a large surface area for heat transfer and thereby causes intense coolant evaporation, which in turn generates pressure waves and dynamic loading to the surrounding structures. While the general understanding of the key physics of the vapor explosion exists, a mechanistic and quantitative description of the governing processes, especially at the micro-interaction (droplet explosion) level, remains elusive. It is therefore instrumental for the droplet vapor explosion to be characterized and studied in detail. Along this line, a test facility named MISTEE (**M**icro **I**nteractions in **S**team **E**xplosion **E**xperiments) was built and operated at the Royal Institute of Technology-Sweden. A novel experimental approach named SHARP (**S**imultaneous **H**igh-speed **A**cquisition of x-ray **R**adiography and **P**hotography) was developed, qualified and employed to characterize dynamics of the melt droplet and vapor bubble during a single droplet vapor explosion. This was accomplished by synchronous imaging of both melt droplet and vapor film by means of high-speed radiographic and photographic imaging, respectively. [1]

The well-controlled single droplet vapor explosion experiments are focused on the characterization of the triggering process, since it is the event that initiates the rapid local heat transfer and pressure rise, which is necessary if a propagating wave is to develop. The complex character of a vapor explosion comes from the fact that many parameters are involved in its triggering, such as physical properties associated with the fuel and coolant, initial fuel and coolant temperatures, ambient pressure, presence of non-condensable gases (NCG), etc. The current study is concerned with the latter parameter, which is realistic for a nuclear reactor severe accident involving MFCIs. For the actual scenario, NCG will be present due to entrapment

during the molten corium jet incursion into the water pool bellow the vessel; as well as due to chemical reactions which are expected in such an oxidizing environment.

Dynamics of the vapor film that surrounds the hot droplet is the basis for the initiation of the intense interaction, since its destabilization and collapse defines the direct coolant-melt contact. Consequently, any changes in the vapor film characteristics, e.g. presence of non-condensable gases, will directly affect the triggering of the vapor explosion.

The damping effect of non condensable gases on vapor explosion was first suggested by Buchanan [2] by means of cushioning high pressures in the melt or coolant. Besides, the initial collapse of the vapor film is dependent on the minimum approach thickness and the deceleration of the interface due to the film pressure rise. So, if the minimum approach thickness is too large or if deceleration (film pressure) is too small due to the effect of NCG, for a given trigger energy, film collapse will not likely occur. [3]

Nelson and Duda [4], when performing single droplet experiments with molten iron oxide, observed that non-condensable gases entrained in the boiling layer surrounding the melt droplet prevented the spontaneous initiation of a steam explosion. Even by selecting the experiments in which the NCG entrapment was negligible, another source was the oxidation of the molten iron and iron oxide leading to H_2 release. Since the reaction occurs on the whole surface of the droplet, the system (melt droplet and film) presented a more spherically symmetric characteristic. Based on the latter, Kim and Corradini [5] and Kim [6] developed a model to study the behavior of the vapor film around the hot droplet. The study showed that the oscillations on the film are diminished enormously with the increase of NCG gas film thickness due to its retardation of the initial heat transfer across the film and damping effect on the pressure fluctuations. Moreover, the NCG would hinder condensation which is instrumental on in the development of vapor/liquid interface instabilities and thus the steam explosion triggering itself.

Akiyoshi et al. [7] studied the influence of entrapped NCG in the vapor film by performing single tin droplet experiments varying the space content above the water surface in the container with an air atmosphere and steam atmosphere. The experiments showed that spontaneous thermal interaction with an air atmosphere generally generated a weaker pressure pulse than that generated in the tests performed with a steam atmosphere. However, the air atmosphere produced less consistent thermal interactions, with the generated pressure varying by more than one order of magnitude. Moreover, in the air atmosphere only part of the tin droplet fragmented, whereas in the steam atmosphere the whole tin droplet was finely fragmented.

Zimanowski et al. [8] performed experiments with molten volcanic rocks containing CO_2 (~15vol.%) rich mineral phases. The CO_2, released into the vapor film, prevented the vapor explosion interaction.

Taleyarkhan [9] performed molten tin experiments in a water pool with and without a gas injection, and found that only benign quenching occurred for the tests with air bubbling through the water. The author also proposed the injection of NCGs in the coolant through a perforated plate for the prevention of steam explosions.

In short, past works have suggested that the non-condensable gases influence the motion of vapor-liquid interfaces, suppressing the vapor film collapse and direct liquid-liquid contact. The NCG are therefore thought to reduce vapor explosion triggerability and energetics. The effect thus offers a way to test the contribution of various mechanisms involved. In this paper, our objective is to present SHARP results and discuss findings from the MISTEE-NCG test campaign.

2. EXPERIMENTAL SETUP

The test facility named MISTEE (**M**icro **I**nteractions in **S**team **E**xplosion **E**xperiments) shown in Fig. 1a is

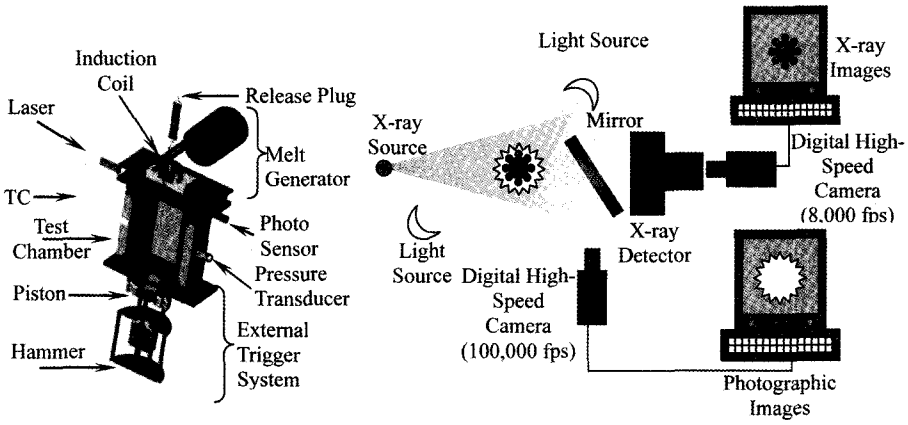

Fig. 1. MISTEE Test Section and SHARP Visualization System

designed for the visualization of the explosion of a single droplet disturbed by a weak pressure wave, characteristic of the early triggering phase in a vapor explosion. The facility consists of a test chamber, a melt generator, an external trigger system, an operational control system, and a data acquisition and visualization system.

The test section is a rectangular Plexiglas tank (180 × 130 × 250mm) in which a piezoelectric pressure transducer is flush-mounted at the center of the test section wall. K-type thermocouples are employed to measure temperatures of the molten droplet in the furnace and the water temperature inside the test section. The melt generator consists of an induction furnace (260V, 40A) and a graphite cylinder (40mm O.D. × 50mm) with an alumina crucible (20mm I.D. × 30mm). A molten tin mass of 0.5-0.7g is loaded to the crucible to guarantee the single-droplet delivery through a 5.0mm hole at the center of the crucible bottom. The melt generator, which includes the induction coils and the melt crucible, is housed inside a chamber into which argon gas is purged in to suppress undesired oxidation reactions during the heating and melting phases. A boron-nitride plug is used to block the hole in the crucible bottom during the melting and this plug is lifted by a pneumatic piston to release the melt droplet. The external trigger system can be described as a piston located at the bottom of the test section, which generates the sharp pressure pulse (rising time of 50 μs at the full width half maximum) up to 0.15 MPa that travels through the coolant. The trigger hammer that impacts on the piston to generate a pressure pulse is aligned underneath the latter, and is driven by a rapid discharge of a capacitor bank, consisting of three capacitors of 400 Vdc and 4700 mF each.

The fast synchronous visualization system, **SHARP** (**S**imultaneous **H**igh-speed **A**cquisition of x-ray **R**adiography and **P**hotography), as shown in Fig. 1b, consists of tungsten lighting and a high speed CMOS digital camera (Redlake HG50LE), up to 100000 fps (with 20000 fps rate used for the MISTEE tests) for the photography; and a continuous X-ray source tube (Philips MCN 321 - max. 320 keV), an X-ray converter, image intensifier and a high speed CCD camera (Redlake MotionScope HR 8000) for radiographic imaging up to 8000 fps. A method to process and synchronize the photographic and X-ray radiographic images acquired was developed and is described in a separate paper [1].

3. NCG - BUBBLE DYNAMICS

A number of MISTEE tests were conducted using molten tin droplet in different water temperatures. The MISTEE-NCG test series was selected among the MISTEE runs in which a considerable amount of air was entrapped with the melt droplet during its plunging through the water's free surface. The entrapped air forms a rear bubble, which varies in size and interacts with the main bubble (vapor film around the droplet). The amount of air confined in the vapor film can then be translated into the bubble morphology, e.g. aspect ratio (width/ height).

Still pictures, recorded by the high speed camera with a temporal resolution of 0.05 ms per frame, are presented in Figs. 2 and 3 revealing the air/vapor bubble progression during its interaction with a 0.6-0.7 g molten tin droplet initially at 1000°C.

In Fig. 2, at first, the undisturbed molten droplet, undergoing stable film boiling along with a large air/vapor rear (aspect ratio: 0.483), falls freely into the water with a velocity of 0.7 m/s. At t=0 ms, the system is disturbed by an external pressure pulse of 0.15 MPa. The pressure wave compresses the bubble that encloses the droplet, as seen at t=0.15ms. Induced by the passage of the pressure wave, the air/vapor rear collapses (t=0.45ms) compressing the contents of the bubble. In this way the NCG content acts as a spring and drives the air/vapor rear back into expansion (t=0.75ms). Thereafter, the rear collapses once more (t=1.15ms).

A small jet appears on the low periphery of the bubble during the first collapse of the rear, at t=0.25ms. Jet formation is commonly observed in cavitation phenomena, in which the asymmetric collapse of the vapor film leads to an elongated shape of the bubble in the downward direction [10,11]. In the present scenario the jet develops in a time scale of 1 frame, i.e. 0.05ms; it then recoils and forms again cyclically.

The parallel oscillatory behavior of the rear and jet carries on until the direct liquid-liquid contact[1] occurs and nucleation takes place, expanding the bubble and rear. The overgrown bubble/rear reaches its maximum size

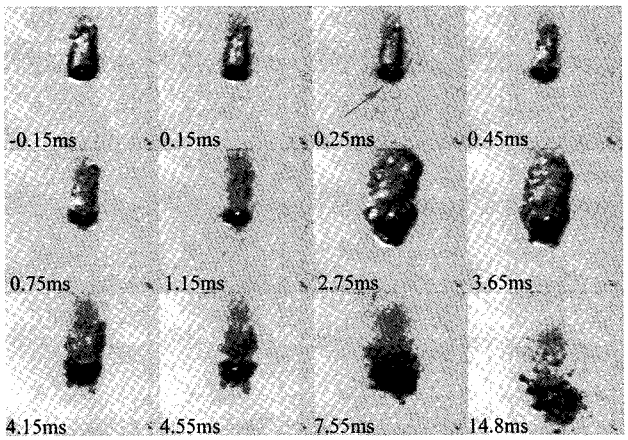

Fig. 2. Photographic Sequence of a Typical MISTEE-NCG Test when a Large Rear (AR<0.6) is Present

[1] In principle a direct liquid-liquid contact is not necessary to initiate such a vapor production, an air/ vapor film may always be present (minimum film approach thickness). [12,13].

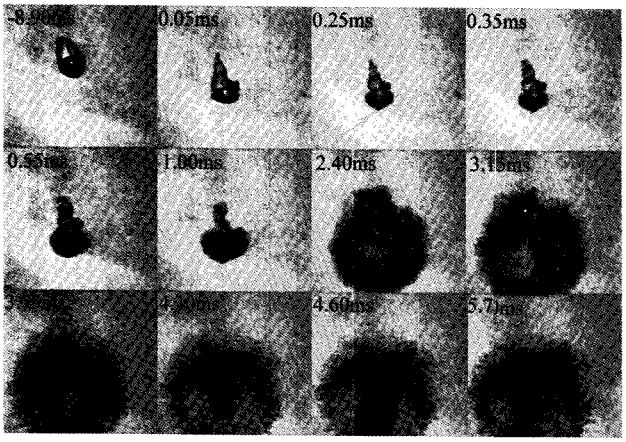

Fig. 3. Photographic Sequence of a Typical MISTEE-NCG Test when a Small Rear (AR≤1) is Present

(t=2.75ms) and starts to collapse towards the molten droplet. The accelerating interface on the rear side hits the molten droplet (t=7.55 ms) adding the NCG into the interaction zone with such a kinetic energy as to hydrodynamically fragment the droplet. Film boiling on the still hot fragments (t=14.8ms) points out to the suppression of the direct melt-coolant contact and thus, the vapor explosion itself.

Fig. 3 shows the bubble/rear evolution for a larger aspect ratio, e.g. less entrapped NCG. Initially, the dynamics are similar to those described in the previous case: air/vapor film collapse, as seen at t=0.05ms, rear oscillatory behavior (t=0.05 to 1ms) and jet cyclic formation underneath the main bubble (t=0.25ms). However, during the last rear collapse (t=1ms) the melt droplet is partially exposed to the coolant in the main bubble lower hemisphere. The mixing, e.g. melt-coolant direct contact, occurs, leading to an explosive vapor generation and fragmentation of the whole droplet (t=1ms to 5.7ms). The fine fragments set off in the radial direction following the interface of the growing bubble (t=2.4ms). As the vapor bubble decelerates, the inertia of the fine fragments causes them to go through the bubble surface (t=3.15ms). The latter reaches its critical size and the subsequent bubble collapse leaves the fine fragments dispersed into the coolant (t=4.30ms).

In Fig. 4, the radial growth history of the vapor bubble, for different coolant temperatures and different aspect ratios, is represented by the normalized equivalent diameter (D_{eq}), estimated by the image projected area.

The MISTEE-NCG data shows that the presence of a significant amount of NCG (aspect ratio<0.6) can suppress the bubble's energetic "second cycle". The mechanism that governs the vapor explosion suppression is the collapsing interface at the end of the first cycle that introduces the NCG into the mixing zone, hindering the direct liquid-liquid contact, which is central to melt-coolant heat transfer and evaporation, Fig. 2.

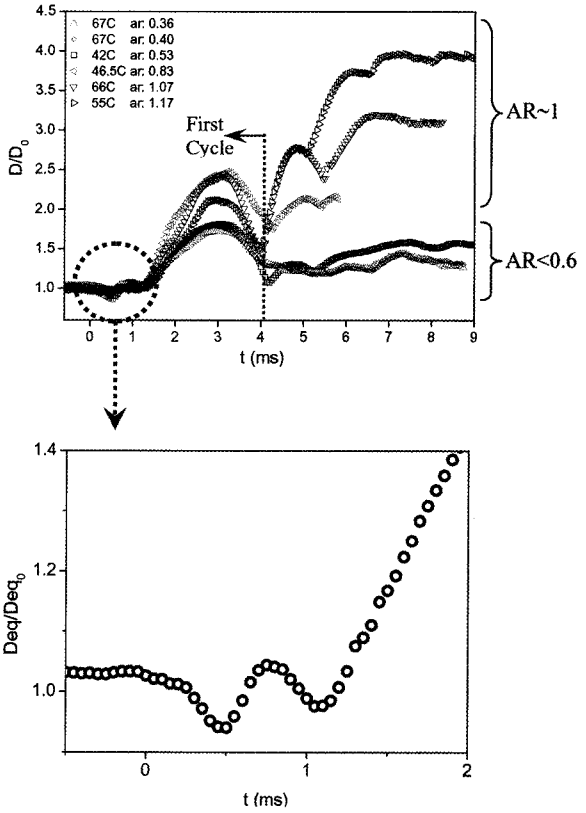

Fig. 4. Dynamics of the Air/vapor Bubble that Enfolds the Melt Droplet and Detail from the Initial Rear Dynamics

Conversely, in the case when there is a relatively small amount of NCG (aspect ratio ≤1) the direct melt-coolant contact occurs during the bubble interface collapse at the end of the first cycle (low subcooling) or during the rear dynamics (high subcooling), Fig. 3, leading to vapor explosion and fine fragmentation of the melt.

Such an energetic interaction diverges greatly from the mild characteristics of the first case. This puzzling finding was the main motivation for scrutinizing the role of NCG on the vapor explosion.

4. BUBBLE- MELT DYNAMICS

The bubble dynamics history provides the integral phenomenology of the vapor explosion; however, it gives no information on the structure of the molten droplet and its fragmentation, which defines the energetics of the vapor explosion process. Therefore, the analysis of the simultaneous X-ray radiography-photography becomes imperative, and is shown below for the two distinctive cases:

4.1 Aspect Ratio <0.6

In Fig. 5, a 0.7g tin droplet, initially at 1000°C, undergoing

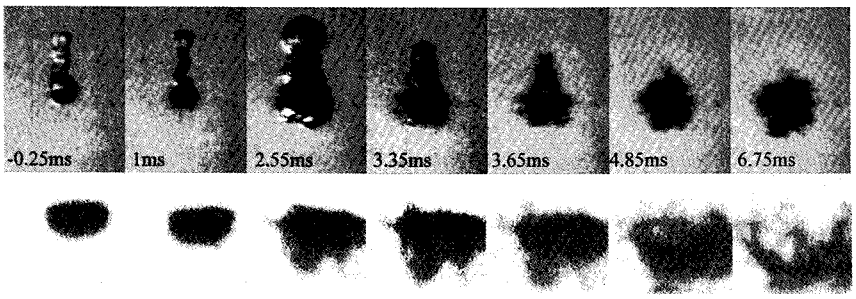

Fig. 5. Simultaneous Photographic and X-Ray Radiography of a Vapor explosion Sequence in the Presence of a Large Rear (AR<0.6)

film boiling with a considerable amount of NGC entrapped on the bubble rear (aspect ratio of 0.347), is descending through the coolant at 38°C. The effect of the coolant temperature is visible on the air/ vapor rear, which is much wavier than the low subcooled cases (Fig. 2).

Between t=0.05ms and 1ms, the bubble air/ vapor rear undergoes contraction/ expansion/contraction. This process leads to a near melt-coolant contact, which causes the bubble to expand (t=1-05ms to 2.55ms). On the melt side, the initially disc-shaped droplet is deformed relatively slowly during the bubble growth phase, forming a substructure on its lower hemisphere.

After reaching its maximum size (t=2.55ms), the air/vapor bubble starts collapsing. The bubble asymmetry during the collapse phase causes one side, e.g. the rear, to accelerate inward more rapidly than the opposite side, resulting in the formation of a localized jet in the final stages of the collapse phase (t=2.65 to 4.85ms). When the coolant impacts on the top side of the melt droplet, the hydrodynamic forces associated with the inrush of water and NCG on the interaction zone shatter the distorted droplet, as clearly seen in the X-ray images (t=4.85ms to 6.75ms).

In the MISTEE-NCG tests that involved a large elongated air/vapor film morphology, e.g. aspect ratio smaller than 0.6, the same bubble and melt dynamics were consistently observed. Hence, for such conditions, independent of the water subcooling, one should expect the suppression of the vapor explosion.

4.2 Aspect Ratio ≤1

Figs. 6 and 7 show the melt-coolant interaction progression for a single tin droplet, initially at 1000 °C, for different water temperatures, 45 °C and 66 °C respectively. The droplet is surrounded by a vapor/air film with morphological aspect ratio of 0.787 and 0.933, respectively.

As in the case of the aspect ratio described previously, AR<0.6, oscillatory dynamics of the air/vapor rear and jet formation on the lower hemisphere during the initial destabilizing phase are also observed on the low subcooled runs (0.05ms to 0.85ms) and on the high subcooled runs (0.05ms to 1ms). During this stage, the droplet is elongated

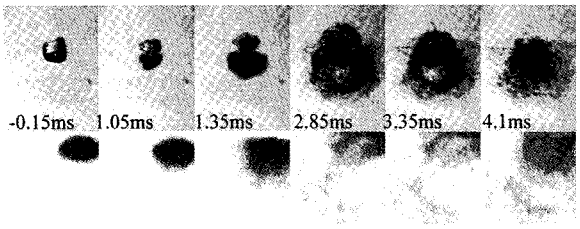

Fig. 6. Simultaneous Photographic and X-Ray Radiography of Vapor explosion Sequence in the Presence of NCG at High Subcooling

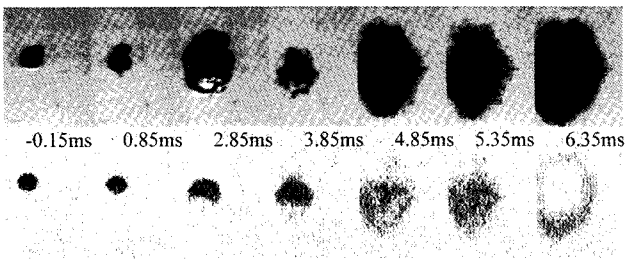

Fig. 7. Simultaneous Photographic and X-Ray Radiography of Vapor explosion Sequence in the Presence of NCG at Low Subcooling

on the lower section, as shown in Fig. 6 (1.05ms) and Fig. 7 (0.85ms).

In the case of higher subcooling, the rear and jet oscillations were sufficient to trigger the vapor explosion by the direct contact of the distorted lower fraction of the droplet with the coolant (t=1.35ms). The turbulent motion of the explosive vapor generation leads to the fine fragmentation of the whole droplet (2.85ms).

In the case of lower subcooling, shown in Fig 7, the last contraction of the oscillating rear leads to the initial heat transfer across the film and subsequent bubble/rear growth. The overgrown bubble reaches its maximum (t=2.85ms) and starts collapsing. At this phase, the already disturbed melt (t=0.85ms) mixes with the coolant, leading to an explosive vapor generation and fine fragmentation in two cycles (4.85ms and 6.35ms).

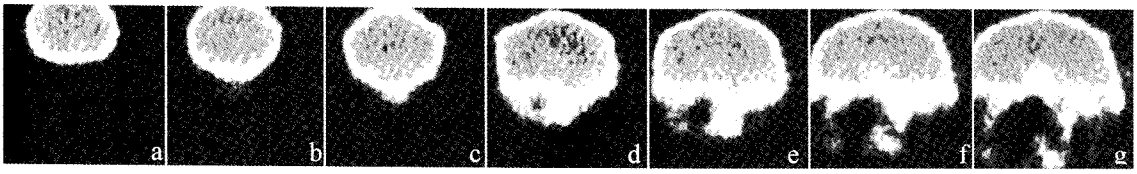

Fig. 8. X-ray Radiography Close-up of the Droplet Undergoing Deformation/Prefragmentation in the Presence of NCGs

Given that the rear has a high content of NCG, it presents an obstacle for coolant entrainment. As a result, in both cases the direct melt-coolant contact, shown in Fig. 6 (1.35ms) and Fig.7 (3.85ms), occurs at the lower hemisphere where the air/vapor film is thinner and more susceptible to instabilities. In fact, during the impact of the collapsing bubble, the droplet substructure is exposed to the coolant while the inrushing water mixes with the disintegrated droplet.

In order to scrutinize any internal structures of the droplet, e.g. the mentioned substructure, close-up X-ray radiographies of a molten droplet undergoing deformation/ prefragmentation were acquired and are shown in Fig. 8.

Initially the droplet has an ellipsoidal shape, as shown in Fig. 8a. After the passage of the pressure wave, the collapsing bubble rear produces a downward air/steam flow, manifested as a jet in lower part of the bubble, which draws off a surface mass layer creating an elongation on the droplet bottom, as shown in Fig.8b.

The independent rear dynamics aggravate the asymmetric pressure distribution, thus building a highly turbulent flow inside the air/ vapor film, which might be responsible for the further droplet disintegration, as shown in Fig 8c. Moreover, the jet recoil and rebound could lead to micro jet penetrations that would cause the indentation of the droplet bottom surface. [14-17]

During the first bubble expansion, shown in Fig. 8d-g, the lower side of the droplet develops so as to become highly convoluted with thin filaments of metal forming a substructure similar to a 'jelly-fish'. The growth of a substructure on the already disturbed droplet occurs probably as a result of the convective flow generated by the bubble expansion. Regardless, such deformation/prefragmentation justifies the frequent occurrence of vapor explosion triggering on the lower hemisphere.

The influence of the coolant temperature on the triggering and fine fragmentation dynamics is apparent when comparing these two cases with different water subcooling. Given that triggering is closely connected with the preceding droplet preconditioning, its analysis is the next natural step.

5. PRECONDITIONING

The concept of preconditioning, introduced by the authors [18], states that the droplet deformation/ prefragmentation during the initial bubble cycle, i.e. up to the first bubble expansion will dictated the vapor explosion energetics. This is to say that the greater the melt droplet's deformation/prefragmentation during this period, the easier it is for the coolant to entrain upon bubble collapse, which will then allow a larger mass of volatile coolant to permeate deeper into the melt interior. The enhanced mixing environment is more favorable to the subsequent energetic explosive vaporization.

Deformation/prefragmentation of a molten droplet can be quantified by its projected area evolution prior to the direct molten-coolant contact, $A_{melt,final}/A_{melt,initial}$. Fig. 9a shows that the droplet preconditioning is independent of the bubble aspect ratio. That can be rationalized since NCG are mostly allocated in the bubble rear; given that evaporation will mainly take place on the lower region of the main bubble; since the upper droplet region is isolated by the rear, the vapor is forced to flow around the droplet, dragging the NCG with it. Therefore, independently of the rear size, the conditions of the bubble on the lower hemisphere, i.e. NCG content, will be similar for the cases with equal coolant temperature.[2]

On the other hand, different coolant temperatures will generally affect the stability of the bubble that envelops the droplet, even with the presence of NCG. There is to say, the higher the coolant temperature, the thicker and more stable the vapor film is. Accordingly, when disturbed by an external trigger, pressure oscillations in the vapor-liquid interface would be damped effectively on a thicker film, resulting in a smaller susceptibility for such external disturbances to propagate to the melt. Therefore, the lower subcooling will result in a more limited deformation/ prefragmentation of the molten droplet, i.e. preconditioning, as shown in Fig. 9b.

While in the runs with a negligible amount of NCG present the same preconditioning trend; the melt deformation/

[2] In experiments with molten iron oxide drops released into water, Nelson and Duda observed that for larger fall distances the drop appeared to pull a small bubble of air along with it. "*The drop always seemed to be located at the bottom of the bag, and to have about the same film thickness beneath it, regardless of the bag above it.*" [4]

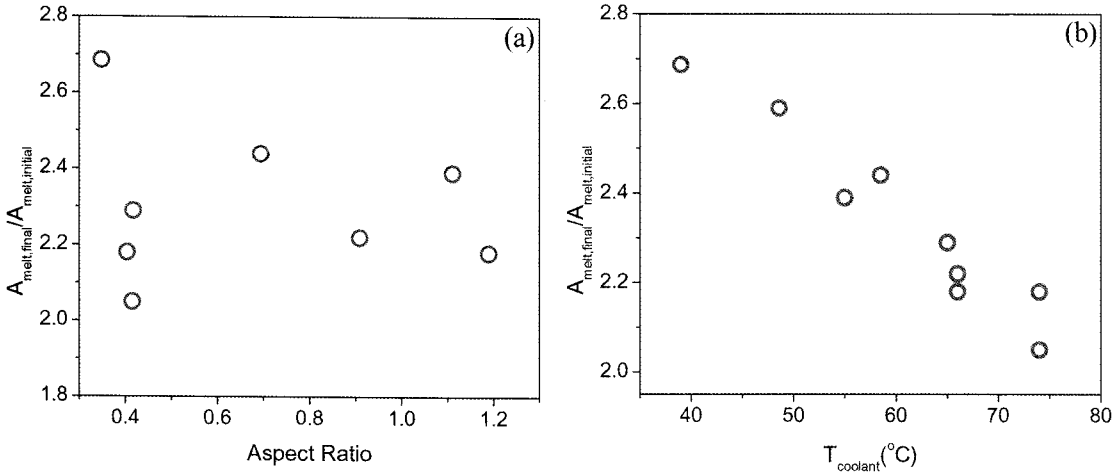

Fig. 9. Molten Droplet Deformation/Prefragmentation Represented by its Projected Area, A_{melt}, in Respect to the Bubble Aspect Ratio (a) and Coolant Temperature (b)

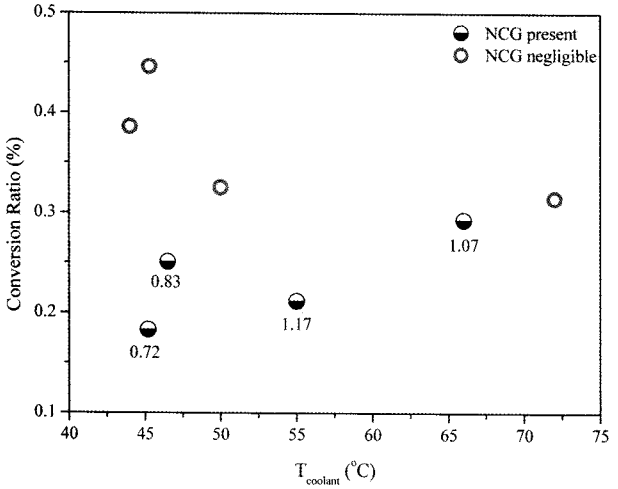

Fig. 10. Conversion Ratio for a Single Tin Droplet Undergoing Steam Explosion in the Presence and Absence of NCG in the Vapor Film. The Aspect Ratio is Indicated for the cases where NCG is Present

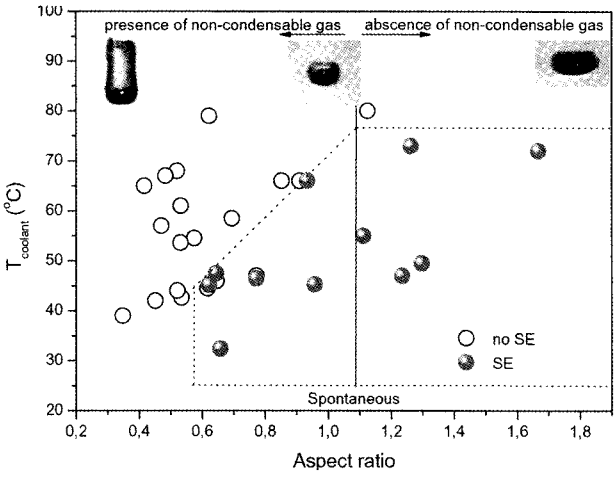

Fig. 11. Thermal Interaction Zone Map

prefragmentation itself takes place in a more uniform manner as compared with the distorted characteristics of the melt droplet in the presence of NCG, as shown in Fig. 8g. This condition is repeatedly observed, thus pointing to a higher preconditioning and consequently enhanced triggerability.

6. ENERGETICS

On one hand the presence of NCG enhances preconditioning; on the other hand it hinders the direct liquid-liquid contact when introduced in the interaction zone. This delicate balance will be defined by the NCG content in the bubble, e.g. the aspect ratio. The resulting energetics for the MISTEE-NCG tests, which underwent vapor explosion, yielded approximately 7 to 50% lower conversion ratios than the MISTEE tests (without NCGs), depending on the aspect ratio, as shown in Fig. 10.

7. CONCLUSION

The previous understanding of the non-condensable gas effect on a vapor explosion was mostly based on the assumption of a symmetric vapor/air film. In such a case, calculations show a damping effect due to the presence of NCG on the interface oscillations (instrumental for the vapor explosion triggering). Moreover, presence of NCG would increase the minimum approach thickness due to

the pressure rise on the film. [3,4]

Observations reported in this paper indicate, however, that the NCGs tend to accumulate in the rear region of the rising film. Such asymmetry leads to complex pressure dynamics governing the bubble's internal flows and jet formation on its interface. The resulting forces and interactions are sufficient to disturb the droplet surface, facilitating its amenability (preconditionability) for the coolant ingression and fine fragmentation, e.g. triggerability. Conversely, the presence of NCGs in the interaction zone hinders the direct melt-coolant contact, lowering the resulting energetics, for which the upper limit for an energetic vapor explosion is found to be for an aspect ratio less than 0.6.

The Thermal Interaction Zone map can then be redesigned by adding the non-condensable gas represented by the vapor/air film aspect ratio, as shown in Fig 11. Yet, the probability of inclusions of NCG in the vapor film remains elusive, thus giving the unjust "stochastic" attribute to the vapor explosion.

The MISTEE data on bubble behavior, including the well-characterized dynamics of NCG rear bubble, can be useful in the analysis of preconditioning and its effect on the subsequent energetics. In particular, advanced methods in computational multi-fluid dynamics (with interface tracking) can be used together with the measured data to determine the evolution of pressure and flow fields in the bubbles, which helps to relate the flow effect on droplet stability, deformation and pre-fragmentation, which are characterized by the X-ray imaging.

ACKNOWLEDGMENTS

This research was supported by the Swedish Nuclear Power Inspectorate (SKI), Swedish Power Companies, Nordic Nuclear Safety Program (NKS), Swiss Nuclear Safety Commission (HSK) and EU SARNET Project. The author is also grateful to Prof. Nam Dinh of the Idaho National Laboratory for the valuable suggestions to improve the manuscript.

REFERENCES

[1] R. C. Hansson, T.N. Dinh, H.S. Park, "Simultaneous High Speed Digital Cinematographic and X-ray Radiographic Imaging of an Intense Multi-Fluid Interaction with Rapid Phase Changes," *Experimental Thermal and Fluid Sciences*, Vol. 33, pp 754-756, 2009.

[2] D. J. Buchanan, "A Model for Fuel-Coolant Interactions," *J. Phys. D: Appl. Phys.*, **7**, (1974).

[3] M. L. Corradini, "Phenomenological Modeling of the Triggering Phase of a Small-Scale Steam Explosion Experiments", *Nucl. Sci. and Eng.*, **78**, (1981).

[4] L. S. Nelson and P. M. Duda, "Steam Explosion Experiments with Single Drops of Iron Oxide Melted with a CO_2 Laser," *High Temperature*, **14**, (1982).

[5] B. J. Kim, M. L. Corradini, "Recent Film Boiling Calculations: Implications on Fuel-Coolant Interactions," *Int. J. Heat Mass Transfer*, **29**, 8(1986).

[6] B. J. Kim, "Oscillatory Behaviors in Initial Film Boiling: Implications on the Triggerability of Single Droplet Vapor Explosions', *KSME Journal*, **3**, 2(1989).

[7] R. Akiyoshi, S. Nishio and I. Tanasawa, "A Study on the Effect of Non-Condensable Gas in the Vapor Film on Vapor Explosion", *Int. J. Heat Mass Transfer*, **33**, 4(1990).

[8] B. Zimanowski, G. röhlich, V. Lorenz, "Experiments on Steam Explosion bu Interaction of Water with Silicate Melts", *Nucl. Eng. and Design*, **155**, (1995).

[9] R. P. Taleyarkhan, "Vapor Explosion Studies for Nuclear and Non-Nuclear Industries," *Nucl. Eng. and Design*, **235**, (2005).

[10] T. B. Benjamin, A. T. Ellis, "The Collapse of Cavitation Bubbles and the Pressures Thereby Produced Against Solid Boundaries," *Philos. Trans. R. Soc. London*, **A260**, 221(1966).

[11] W. Lauterborn, C. D. Ohl, "The Peculiar Behavior of Cavitation Bubbles," *Applied Scientific Research*, **58**, (1998).

[12] G. Ciccarelli, "Investigation of Vapor Explosions with Single Molten Metal Drops in Water Using Flash X-ray," Ph.D. Thesis, McGill University, Canada (1991).

[13] J. Lamône, R. Meignen, "Analysis of the Thermal Fragmentation as a Mechanism for the Initiation of Steam Explosion," *Proceedings of International Congress on Advances in Nuclear Power Plants (ICAPP 7)*, Nice, France, May 13-18, 2007.

[14] M. H, Cunningham and D. L.Frost, "Effect of Coolant on the Fragmentation of Single Melt Drops in Water", *Proc. of 8th International Topical Meeting on Nuclear Reactor Thermohydraulics (NURTEH-8)*, Kyoto, Japan, September 30-October 4, 1997.

[15] S. J. Board, C. L. Farmer, D.H. Poole, "Fragmentation in Thermal Explosions," *Int. J. Heat and Mass Transfer*, **17**, 2(1974).

[16] M. S. El-Genk, R. B. Matthews, S. G. Bankoff, "Molten-Fuel Coolant Interaction Phenomena with Application to Carbide Fuel Safety," *Progress in Nuclear Energy*, **20**, 3(1987).

[17] C. D. Ohl, R. Ikink, "Shock-Induced Jetting of Micron-Size Bubbles," *Physical Review Letters*, **90**, 21(2003).

[18] R. C. Hansson, T. N. Dinh, H. S. Park, "Dynamics and Preconditioning in a Single Droplet Vapor Explosion," *Nuclear Technology*, Vol. 167, pp 223-234, 2008.